Food Chemistry 481 (2025) 144036

Contents lists available at ScienceDirect

Food Chemistry

journal homepage: www.elsevier.com/locate/foodchem

The transepithelial transport of peptides derived from insects (*Galleria mellonella* and *Alphitobius diaperinus*) through static *in vitro* digestion (INFOGEST) and their ability to mitigating oxidative stress

Zidan Ma [a], Martin Mondor [b,c,d], Christine Boesch [a], Oscar Abel Sánchez-Velázquez [a], Adam A. Dowle [e], Alan Javier Hernández-Álvarez [a,*]

[a] Food Science and Nutrition, University of Leeds, Leeds LS2 9JT, UK
[b] Saint-Hyacinthe Research and Development Centre, Agriculture and Agri-Food Canada, Saint-Hyacinthe, QC J2S 8E3, Canada
[c] Department of Chemical Engineering and Biotechnological Engineering, Université de Sherbrooke, Sherbrooke, QC J1K 2R1, Canada
[d] Institute of Nutrition and Functional Foods (INAF), Université Laval, Quebec, QC G1V 0A6, Canada
[e] Bioscience Technology Facility, Department of Biology, University of York, York YO10 5DD, UK

ARTICLE INFO

Keywords:
Galleria mellonella
Alphitobius diaperinus
INFOGEST
Transepithelial transport
Insect permeable peptides
Peptide identification
Antioxidant

ABSTRACT

Insect protein-derived peptides are gaining attention for their potential bioactivities. This study aimed to evaluate the antioxidant ability of peptides derived from gastrointestinal digestion and assess their absorption through transepithelial transport. Results indicate an increase of antioxidant properties from *G. mellonella* (W) and *A. diaperinus* (B) proteins, including reducing power (Fe^{2+}, Cu^{2+}) and radical scavenging (ABTS, DPPH) with enhanced antioxidant activities in gastrointestinal digestates compared to gastric digestates. The inhibition of intracellular Reactive Oxygen Species (ROS) confirmed these findings, the inhibition rates of 40.2 % (W) and 58.5 % (B), respectively. Transepithelial transport analysis demonstrated that peptide absorption primarily occurred between 6 h and 24 h, with W exhibiting a higher apparent permeability coefficient (6.10×10^{-6} cm/s) compared to B (5.91×10^{-7} cm/s). The results highlight the antioxidant potential and absorption capability of insect-derived peptides, with W demonstrating superior antioxidant activity in most assays, whereas B proved more effective in inhibiting intracellular ROS. These findings support the potential of both W and B as bioactive ingredients with functional applications.

1. Introduction

Food-derived bioactive peptides have garnered significant interest due to their potential health-promoting effects (Araiza-Calahorra et al., 2022; Udenigwe & Aluko, 2012). Among these, insect-derived peptides are steadily gaining popularity given that insect proteins are increasingly regarded as sustainable alternatives (Ma et al., 2023). However, the stability of food-derived bioactive peptides during the digestion remains a major limitation. The low stability is often attributed to hydrolysis by digestive enzymes, which can diminish or entirely negate their bioactivities (Amigo & Hernández-Ledesma, 2020). Additionally, peptides are susceptible to degradation by brush border enzymes, i.e. membrane-bound peptidases located on the surface of enterocytes. Factors such as peptide length, primary and secondary protein structure, hydrophobicity/lipophilicity, and charge influence peptide absorption (Amigo & Hernández-Ledesma, 2020). While digestion generates numerous bioactive peptides, identifying and selecting those that not only form during digestion stage but also remain intact and bioactive after absorption is essential. These preserved peptides can enter the systemic circulation and be delivered to target organs or tissues, where they exert their functional effects.

Oxidation, a fundamental aspect of cellular metabolism, often leads to the production of free radicals, which can cause oxidative stress and damage (Pizzino et al., 2017). Oxidative damage to lipids, proteins and DNA compromises cell membrane functionality and enzyme activity and has been linked to chronic conditions such as diabetes, cardiovascular diseases (CVD) and cancer (Seifried et al., 2007). While endogenous antioxidant systems – such as glutathione, superoxide dismutase (SOD) and glutathione peroxidase (GPX) - help counteract oxidative stress (Finkel & Holbrook, 2000), dietary antioxidants, including food-derived

* Corresponding author.
E-mail address: a.j.hernandezalvarez@leeds.ac.uk (A.J. Hernández-Álvarez).

https://doi.org/10.1016/j.foodchem.2025.144036
Received 7 December 2024; Received in revised form 19 March 2025; Accepted 23 March 2025
Available online 27 March 2025

peptides, can complement these systems by mitigating oxidative damage. Antioxidants act through various mechanisms, including hydrogen atom transfer, electron transfer and transition metal chelation (Kotha et al., 2022; Prior et al., 2005). Previous studies have reported the generation of antioxidant peptides from various mammalian sources such as porcine and bovine cartilage, fish collagen, and milk casein. However, concerns regarding disease transmission, allergenicity and dietary restrictions limit their application in food products (Xiang et al., 2023). Additionally, some animal-derived peptides exhibit strong undesirable flavors or odors, such as the fishy smell associated with marine peptides, requiring masking or removal strategies (Wang et al., 2023). As a more sustainable option, plant proteins have also been recognized as sources of antioxidant peptides. However, compared to animal-derived peptides, plant-derived peptides typically have higher molecular weights, which can hinder their absorption into the blood stream (Abeyrathne et al., 2022). While peptides derived from insect proteins remain relatively less studied, insect proteins are highly digestible, facilitating peptide production through digestion. Moreover, insect-derived peptides may be more acceptable for individuals with dietary restrictions, as they provide an alternative to conventional animal-based sources.

Previous research highlighted the nutritional and structural properties of insect proteins, specifically Buffalo worm (*Alphitobius diaperinus*) and Waxworm (*Galleria mellonella*). Comprehensive analyses of protein concentrates from both insects revealed their promising protein content and yields suitable for industrial production, exhibiting high *in vitro* protein digestibility (IVPD, 83.6 %) and *in vitro* protein digestibility-corrected amino acid score (IVPDCAAS, 62.7 %) (Ma, Mondor, Dowle, et al., 2024). Similarly, waxworm protein concentrate was recommended for its superior IVPDCAAS (54.9 %) and IVPD (76.3 %) values (Ma, Mondor, Goycoolea, et al., 2024). Building on these findings, the current study sought to investigate the release of peptides from waxworm and buffalo worm proteins during simulated human gastrointestinal digestion and their absorption. The INFOGEST model was combined with an intestinal Caco-2 monolayer absorption model to simulate gastrointestinal digestion and peptide absorption in the human body. Furthermore, peptides generated during digestion were evaluated for their antioxidant activities, and peptides permeable through Caco-2 cells were identified. These results provide robust evidence that insect protein hydrolysates have potential health benefits, underscoring their viability as functional food ingredients.

2. Materials and methods

2.1. Materials

Live waxworms (*Galleria mellonella*) were purchased from a commercial supplier (Livefood4u, Sheffield, UK). Frozen buffalo worms (*Alphitobius diaperinus*) were purchased from the company (Kiezebrink, Suffolk, UK). Following a cryogrinding and defatting step, proteins were extracted by alkaline solubilization followed by isoelectric precipitation and lyophilized for further use (Ma, Mondor, Dowle, et al., 2024; Ma, Mondor, Goycoolea, et al., 2024).

2.2. In vitro digestion (INFOGEST)

The *in vitro* digestion of freeze-dried proteins was performed according to the static INFOGEST procedure with modifications, flowchart is shown below (Fig. 1) (Brodkorb et al., 2019). In brief, 4 × two grams of protein concentrates were weighed separately into tubes, with samples labeled as gastric phase 1 h (G1h), gastric phase 2 h (G2h), gastrointestinal phase 1 h (I1h) and gastrointestinal phase 2 h (I2h). Then, simulated salivary fluid (SSF, 1.6 mL), 0.3 M $CaCl_2$ (1.5 mM in SSF), amylase (75 IU/mL), water + acid/base to adjust pH to 7 were added and the mixture was incubated at 37 °C for 2 min. Next, the gastric phase fluids (SGF), 0.3 M $CaCl_2$ (0.15 mM in SGF), pepsin (2000 U/mL), water + acid/base were added to adjust pH. The samples were again incubated at 37 °C and after 1 h incubation, G1h sample was

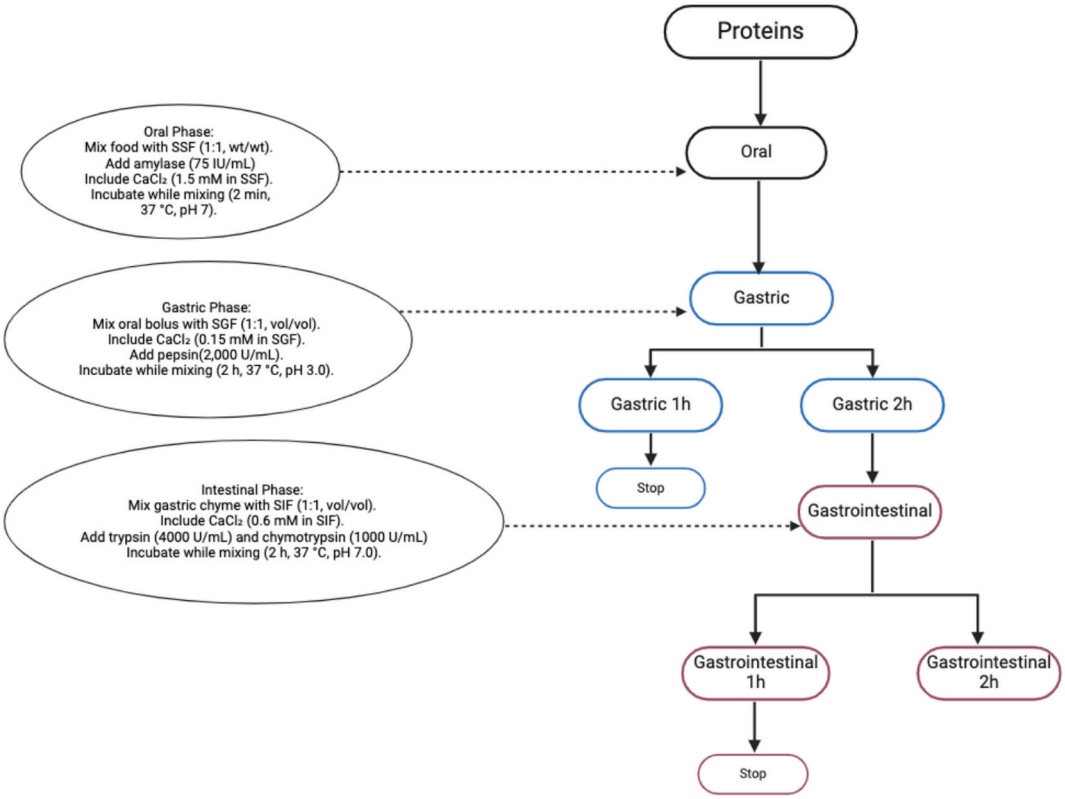

Fig. 1. Flowchart of INFOGEST digestion protocol steps used in this study.

recovered and the pH adjusted to 7 to inactivate the pepsin activity. After 2 h, the G2h sample was subjected to the same treatment. Then gastrointestinal phase fluids (SIF, 5.6 mL), trypsin (4000 U/mL) and chymotrypsin (1000 U/mL), 0.3 M $CaCl_2$ (0.6 mM in SIF), water + acid/base were added to adjust pH of the I1h and I2h digestates; however, lipase, co-lipase, amylase and bile salt solution were excluded (the volume of these were replaced by SIF). The mixtures were incubated at 37 °C for 2 h, I1h was incubated for 1 h, and after the first hour, the I2h sample would undergo an additional hour of incubation. The aliquots were placed on ice after collection (I1h sample and I2h sample); the pH of I2h was checked and adjusted to pH 7 again after gastrointestinal 1 h digestion. To terminate enzymatic reactions, all digestates were incubated at 70 °C for 10 min. Subsequently, the samples were centrifuged at 4500 x *g* for 15 min, and the supernatants ultrafiltrated (Pierce™ Protein concentrator PES, Thermo Fisher Scientific, Loughborough, UK). The fractions below 10 kDa were kept for further analyses and soluble protein content was determined by BCA assay (Thermo Fisher Scientific).

2.3. Degree of hydrolysis

The degree of hydrolysis (DH) was measured according to the TNBS method (Gruppi et al., 2022). In brief, a L-leucine standard curve (Con. 0, 0.25, 0.5, 1, 2, 3 mM) was prepared. Then, 25 μL sample/leucine standard, 200 μL 0.02 % TNBS solution and 200 μL 0.2125 M PBS, pH 8.2 were mixed and incubated for 60 min at 50 °C in the dark. The reaction was stopped by the addition of 400 μL 0.1 N hydrochloric acid and the sample was left for equilibration at room temperature (RT) for 30 min. Then 200 μL of the reaction volume were transferred into wells of a 96-well plate and its absorbance was measured at 340 nm. The total peptide bonds per unit weight were determined according to Hall et al. (2017); in this study, for W is 7.79 and B is 7.89.

2.4. Peptide content

The peptide content of the gastrointestinal digestates was determined using a quantitative fluorometric peptide assay (ThermoFisher). Ten μL sample or standard were combined with 70 μL assay buffer and 20 μL peptide reagent in wells of a black 96 well plate and incubated at RT for 5 min. The fluorescence was measured with Tecan SPARK 10 M Multimode Microplate Reader (Switzerland) with Ex/Em at 390/475 nm. A peptide digest reference standard provided in the kit was used in a concentration range between 0 and 500 μg/mL.

2.5. In vitro antioxidant assays

2.5.1. Iron chelating activity

The iron chelating activity of the digestates was measured according to Carrasco-Castilla et al. (2012) and Canabady-Rochelle et al. (2015) with slight modifications. In brief, 25 μL of digestates (1:20; 1:40; 1:60; 1:80; 1:100; 1:160 dilution) and 225 μL sodium acetate buffer (100 mM, pH 4.9) were mixed with 30 μL iron solution ($FeCl_2$ $4H_2O$, 0.18 mM). Then 12.5 μL of 40 mM ferrozine solution were added to each well and incubated for 10 min at RT followed by absorbance recording at 562 nm. The iron chelating activity of 0.01 μg/mL EDTA was used as a control, and sodium acetate buffer (100 mM, pH 4.9) without digestate or EDTA was used as blank. The iron chelating rate was calculated as below:

$$\text{Iron chelating rate (\%)} = (Abs_{blank} - Abs_{sample}/Abs_{blank}) \times 100.$$

2.5.2. Copper chelating activity

The copper chelating activity of digestates was measured according to Carrasco-Castilla et al. (2012) and Canabady-Rochelle et al. (2015) with slight modifications. In brief, 20.5 μL of digestates (1:20; 1:60; 1:80; 1:100; 1:160 dilution) and 185 μL of sodium acetate buffer (50 mM, pH 6.0) were mixed with 15 μL of copper solution ($CuSO_4$ $5H_2O$, 0.79 mM), followed by addition of 9 μL of pyrocatechol solution (2.00 mM) and incubation for 10 min at RT under light protection. The absorbance was measured at 632 nm using a SPARK 10 M plate reader. The copper chelating activity of 0.01 μg/mL EDTA was used as a control and sodium acetate buffer without digestates/EDTA was used as blank. The copper chelating rate was calculated as below:

$$\text{Copper chelating rate} = ((Abs_{blank} - Abs_{sample})/Abs_{blank}) \times 100.$$

2.5.3. ABTS scavenging activity assay

The ABTS assay was performed according to Re et al. (1999) and Han et al. (2021). In brief, the ABTS (2,2′-Azino-di-[3-Ethylbenzthiazolin sulfonate]) radical stock solution was diluted with MQ-water until its absorbance was 0.700 ± 0.02 at 734 nm. The standard solution was 1000, 750, 500, 250, 100, 50 and 0 μM Trolox in H_2O/ethanol (75:25 *v*/v), the blank was a H_2O/ethanol (75:25 v/v) solution. Then, 10 μL standard/blank/samples (1:20; 1:40; 1:60; 1:80; 1:100; 1:160 dilution) were mixed with 300 μL diluted ABTS radical stock solution and the absorbance was immediately measured (0 min) and after 6 min at 734 nm. The percent of ABTS inhibition was calculated as follow:

$$\text{\% Inhibition} = [(Abs_{\text{sample 0min}} - Abs_{\text{sample 6 min}})/(Abs_{\text{sample 0min}} - [(Abs_{\text{blank 0min}} - Abs_{\text{blank 6min}})/Abs_{\text{blank 0min}}]] * 100.$$

2.5.4. DPPH scavenging activity assay

DPPH radical scavenging activity was performed according to Njoya (2021), Sánchez-Velázquez, Cuevas-Rodríguez, et al. (2021), Sánchez-Velázquez, Mulero, et al. (2021), and Sánchez-Velázquez, Ribéreau, et al. (2021). In brief, 125 μL digestates (1:20; 1:40; 1:60; 1:80; 1:100 dilution) were mixed with 125 μL DPPH solution (0.1 mM in methanol), and were incubated at 37 °C for 10 min and the absorbance was measured at 517 nm. 10 μg/μL Butylated hydroxytoluene (BHT 10 μg/μL, dissolved in methanol) was used as control, and methanol without digestates/BHT was used as blank. The scavenging effects were calculated as:

$$\text{Scavenging effects} = (Abs_{blank} - Abs_{sample})/Abs_{blank} \times 100.$$

2.6. Cell bioactivity

2.6.1. Caco-2 cell culture

The human colon carcinoma cell line Caco-2 was purchased from the European collection of authenticated cell cultures (ECACC) and cultivated in Dulbecco's modified eagle medium (DMEM) containing 4.5 g/L D-Glucose and pyruvate with 10 % FBS, 1 % non-essential amino acids and 1 % penicillin-streptomycin. The Caco-2 cells were routinely grown at 37 °C, in a 5 % CO_2 humidified atmosphere until 80 % confluence was obtained.

2.6.2. Cell viability assay

The cell viability was determined using MTS assay according to the manufacturer's instructions (Promega, Madison, USA). In brief, Caco-2 cells were seeded at a density of 2.2×10^5 cells per well in 96 well plates and grown until 90 % confluent. Then the medium was exchanged by DMEM containing G1h, G2h, I1h and I2h in six concentrations (31.25, 250, 500, 1000, 2000, 3000, 4000, 5000 μg soluble protein /mL). Medium control cells as well as blank control wells received 100 μL DMEM medium only. Following a 24 h incubation, 20 μL CellTiter 96 A_{queous} One solution was directly added to each well and incubated for 4 h, with the absorbance measured at 490 nm using plate reader. Cell viability (%) was calculated by dividing the absorbance reading of hydrolysates and control cells.

2.7. Cellular antioxidant activity assays

2.7.1. Cellular antioxidant activity (CAA)

The cellular antioxidant activity was analyzed according to Kellett

et al. (2018). Caco-2 cells were seeded at 6 × 10^5 per well in 96 well plates (black with transparent bottom), and grown until confluent. The medium was removed, and the cells were washed with DPBS, then the hydrolysates from the end of the gastric and gastrointestinal phases were diluted to different concentrations (31.25, 62.5, 125, 250, 500, 1000 μg/mL soluble protein) with FBS-free DMEM medium. 50 μL of the resulting solutions along with 50 μL 25 μM DCFH-DA working solution were added into each well and incubated at 37 °C in a 5 % CO_2 humidified atmosphere for 1 h. 50 μL DMEM medium (FBS free) mixed with 50 μL DCFH-DA were used as the control, and 100 μL DMEM medium (FBS free) were used as blank. AAPH (100 μL, 600 μM in HBSS) were then added on top after incubation and the absorbance was measured using a Tecan (SPARK 10 M, Multimode Microplate Reader, Switzerland) at ex/em 485/538 nm for 1 h in 5 min intervals (Sánchez-Velázquez, Mulero, et al., 2021). The percent of CAA unit was calculated by the area under the curve (AUC) and the EC_{50} was calculated by the log (CAA unit/100-CAA unit) versus log(dose) as follow:

$$\text{CAA unit} = (1 - (AUC_{sample})/(AUC_{control})) \times 100.$$

2.7.2. Intracellular reactive oxygen species (ROS) quantification

The intracellular ROS scavenging activity was quantified according to Żyżelewicz et al. (2016) with modifications. In brief, the Caco-2 cells were seeded at 6 × 10^5 per well in 96 well black transparent bottom plates, until 80 % confluence was reached. Then the medium was removed and replaced by insect digestates diluted to 2.0, 1.75 and 1.5 mg/mL in DMEM (FBS free). After 24 h of incubation, the digestates were removed and cells washed with DPBS, and subsequently incubated with 2 μL 1 mM DCFH-DA probe in DMEM (FBS free) medium for 30 min. Before inducing oxidative stress, DCFH-DA was removed and the cells were washed by DPBS again, then the cells were induced by 1 mM H_2O_2 (in DMEM FBS free medium) for 3 h, and the fluorescence reading was carried out at ex/em 485/530 nm for up to 3 h in 10 min intervals. The negative control was the fluorescence reading of cells without H_2O_2 treatment, and the control consisted of H_2O_2 treatment with no antioxidant or sample treatment.

2.8. Peptide transepithelial transport

The transepithelial transport of peptides by human Caco-2 cells was conducted according to Hubatsch et al. (2007). In brief, the Caco-2 cells were seeded at 3 × 10^5 in a permeable filter with 1 μm pore size (Tissue culture insert, Sarstedt, Germany) as described for 21 days growth. Then the permeability of the Caco-2 cells tight junction was measured by TEER value (MERSSTX01, Milipore, USA), the TEER value of each well >300 before measurement. The Caco-2 cells monolayer was washed twice and was incubated with HBSS for 30 min before the measurement. Then, the apical side was replaced by 2 mg protein/mL I2h in 0.5 mL HBSS, the basolateral side was replaced by 1.5 mL fresh HBSS and the incubation was carried-out at 37 °C in a 5 % CO_2 humidified atmosphere for 30 min, 2 h, 6 h and 24 h. Then the peptide contents of the apical and the basolateral side were measured using a Quantitative Fluorometric Peptide Assay kit (Thermo Fisher).

The apparent permeability coefficient (P_{app}) was calculated according to Yang et al. (2017):

$$P_{app} = \frac{V_R}{A \times C_0} \times \frac{dC}{dt}$$

where V_R is the volume in the receiver chamber (mL), A is the filter surface area (cm^2), C_0 is the initial donor concentration (apical side) of the peptides (μg/mL), and dC/dt is the initial slope of the cumulative concentration (μg/mL) in the receiver chamber with time (second).

2.9. Peptide identification

The peptides collected from the end stage of gastrointestinal digestion (2 h) and basolateral side (at 6 h and 24 h transport) were analyzed by DDA-PASEF, LC-MS/MS acquisition at the University of York. Briefly, a 2 μg aliquot of each sample was loaded onto EvoTip One tips for desalting and HPLC introduction. Peptides were separated over a 60SPD gradient using an EvoSep One UPLC. Data were acquired using a Bruker timsTOF HT mass spectrometer. For database searching, MS data in .d format were processed and searched using FragPipe (v21.1), with non-specific enzymatic cleavage. All matched peptides were filtered to 1 % FDR and a minimum probability of 0.99. Peptidomic mass spectrometry data sets and results files are referenced in ProteomeXchange (PXD058652) and available to download from MassIVE (MSV000096604) [doi:10.25345/C5JQ0T67Q]. Pre-publication access can be obtained with the following link ftp://MSV000096604@massive.ucsd.edu, username = MSV000096604, password = WR0lqYAk VemOFVBj

2.10. Statistical analysis

All the experiments were carried out in triplicate using the same batch of digestates, and the data are expressed as mean ± standard deviation. Statistical analysis was performed using OriginPro 2021 (Version 9.8.0.200 OriginLab Corporation, Northampton, MA, USA). Significant differences between groups were determined using Tukey's test, with a significant threshold of $p < 0.05$. All graphical representations were plotted using OriginPro 2021.

3. Results and discussion

3.1. Indicators of protein digestibility in insect proteins

Gastrointestinal protein hydrolysis generates a diverse range of protein fragments with varying lengths and properties. As shown in Fig. 2, the kinetics of peptide release was reflected by increases in the degree of hydrolysis (DH), soluble protein and peptide content during both gastric (G1h, G2h) and gastrointestinal (I1h, I2h) digestion phases. Furthermore, the two insect proteins exhibited different behavior during these phases of *in vitro* gastrointestinal digestion. However, for both insect proteins, a general trend of increasing soluble protein content, DH and peptide content with digestion time was observed. For W proteins, digestion during the gastric phase was limited (Fig. 2A). The majority of hydrolysis occurred between G2h to I1h, with soluble protein content increasing by 32.4 % and DH rising by 20.4 % compared to G2h (Fig. 2A). Conversely, digestion activity stabilized between I1h and I2h. Similarly, B proteins displayed the highest DH between G2h to I1h (Fig. 2B), with DH and peptide content increasing by 23.4 % and 64.4 %, respectively. After I1h, these values plateaued during the transition to I2h. The observed differences between the increases in peptide content and soluble protein content during the gastrointestinal phase may be attributed to the limitations of the BCA protein assay. This assay is less effective at detecting small molecular weight components, such as single amino acids and dipeptides (<2000 Da). Consequently, a more pronounced increase in peptide formation was observed during the gastrointestinal phase.

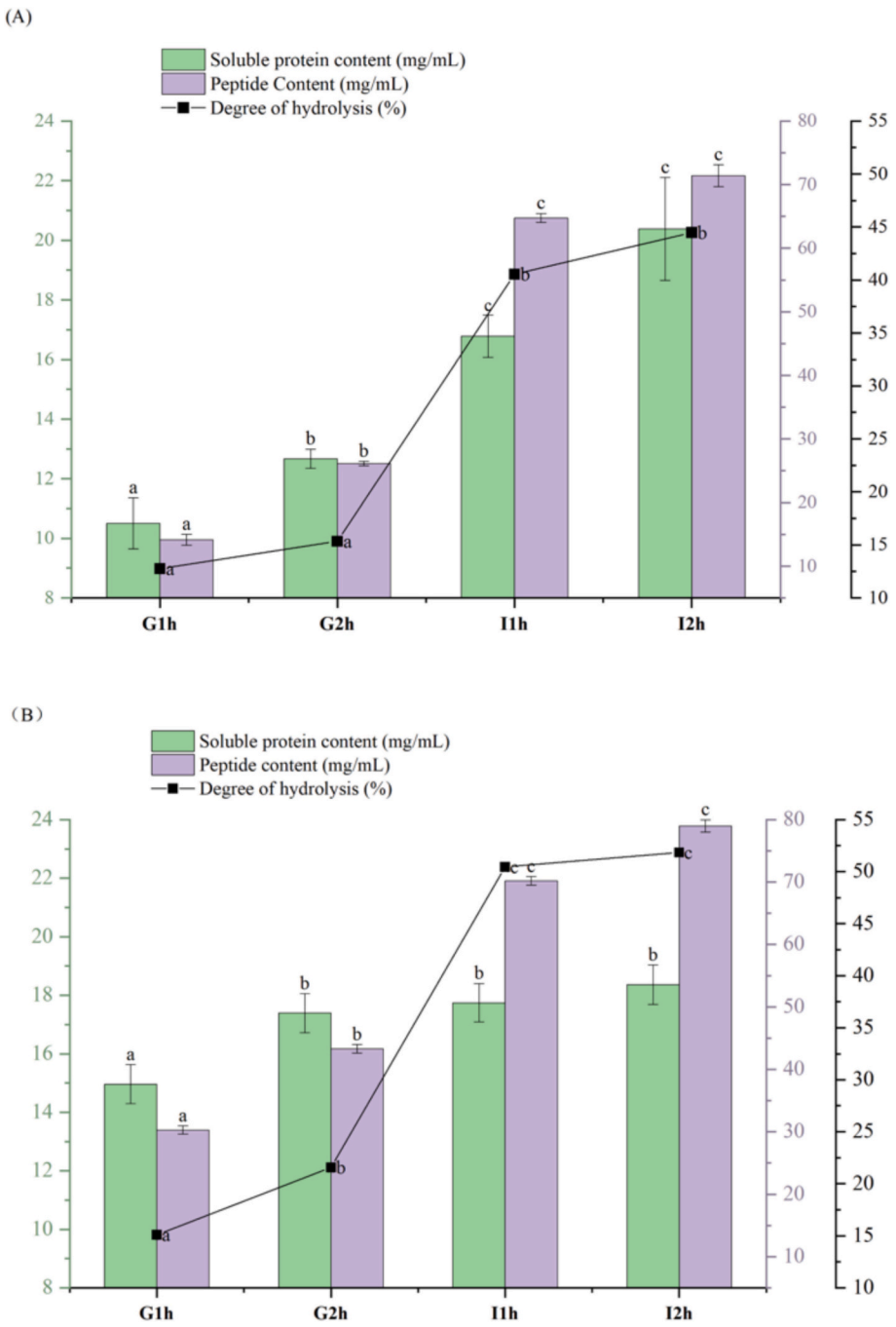

Fig. 2. The gastrointestinal digestion kinetics of (A) Waxworm and (B) Buffalo worm proteins, quantified by soluble protein content (mg/mL), peptide content (mg/mL) and degree of hydrolysis (%). Different letters within each marker indicate significant differences, $p < 0.05$, Tukey test. Data are mean with SD of triplicate experiment.

3.2. Change of antioxidant activities during insect protein digestion

3.2.1. Iron and copper chelating activity

Iron and copper chelating assays are both based on the mechanisms of transition metal chelation. The iron chelating assay evaluates the antioxidants' ability to donate electrons, reducing Fe^{3+} to Fe^{2+}. Excessive Fe^{2+} and Cu^{2+} ions in biological systems can catalyze the generation of reactive oxygen species (ROS), exacerbating oxidative stress. Fe^{2+} ions, for example, react with hydrogen peroxide (H_2O_2) to generate highly reactive hydroxyl radicals (·OH), which exhibit potent oxidative properties. Prior to evaluating oxidative damage *in vivo* or intracellular ROS scavenging ability of insect digestates, the chelating capacities for transition metals Fe^{2+} and Cu^{2+} were assessed.

As shown in Fig. 3, the iron chelating ability of W and B digestates was concentration-dependent, with the strongest effects observed at the highest concentrations. However, both digestates exhibited lower iron chelating activity compared to 0.01 μg/μL EDTA control, except for W-I1h (10,500 μg/mL) which showed the highest iron chelating rate at 48.1 %. The iron binding capacity of chelators is influenced by the functional groups involved in chelation. Siderophores with three bidentate ligands form hexadentate complexes, representing the most efficient chelating structures (Roosenberg et al., 2000). Antioxidants with single ligands can also chelate ferric ions, but with reduced capacity compared to tri-bidentate ligand structures. The common binding

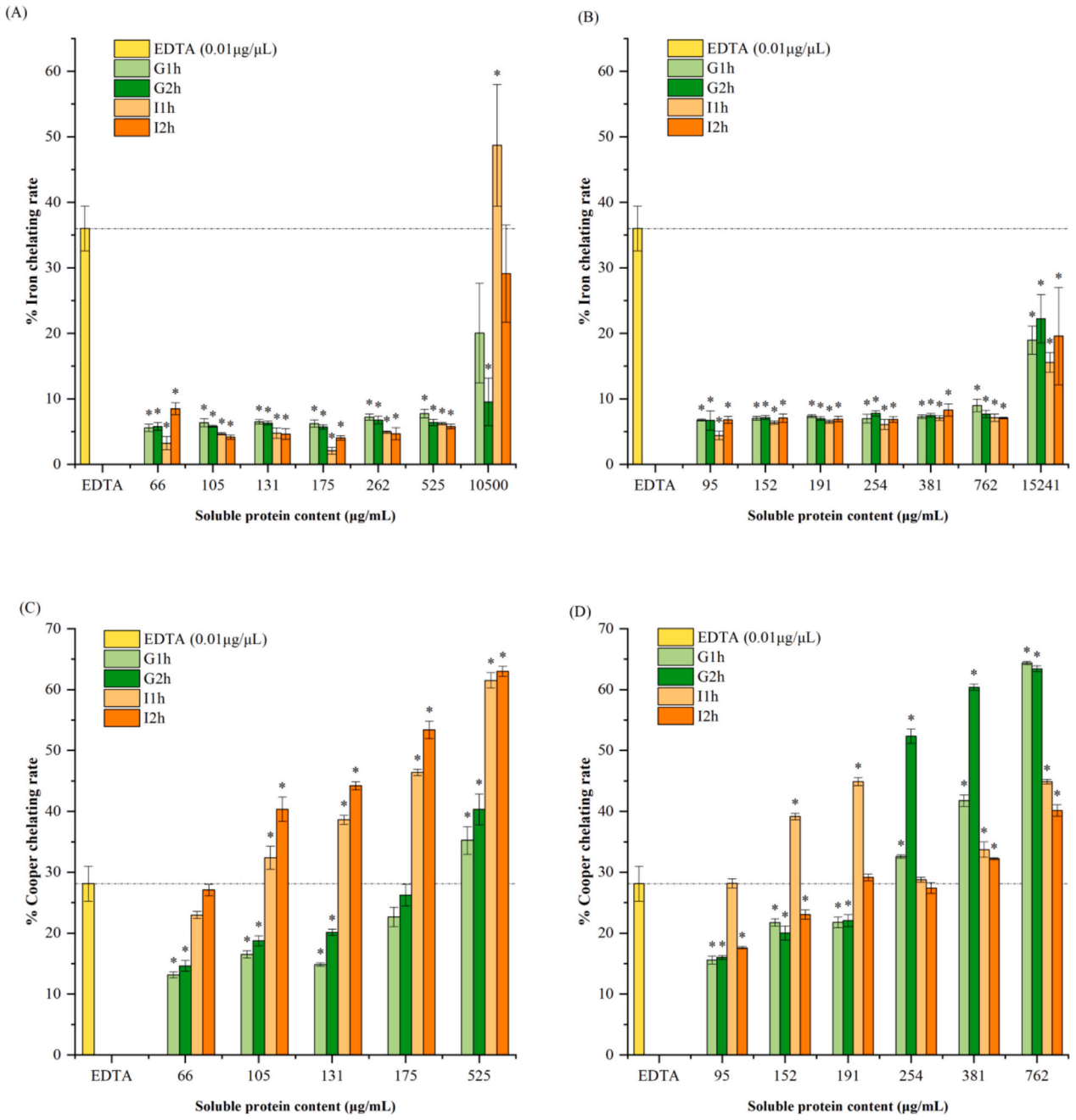

Fig. 3. Iron chelating rate (%) of (A) Waxworm protein digestates and (B) Buffalo worm protein digestates derived from gastric and intestinal phases 1 h and 2 h (G1h, G2h, I1h, I2h). Copper chelating rate (%) of (C) Waxworm protein digestates; and (D) Buffalo worm protein digestates derived from gastric and intestinal phases 1 h and 2 h (G1h, G2h, I1h, I2h).* Means significant difference ($p < 0.05$) compared to the EDTA (0.01 μg/mL) control, Tukey test. Data are mean with SD of triplicates.

sites are carboxylate, imidazole and phenolic hydroxyl groups (Roosenberg et al., 2000). Thus, peptides from W-I1h can possibly form bidentate (bind at two site) or tridentate, forming highly stable chelation rings around the iron and enabling their high iron chelating activity. Similar peptide-binding properties have been reported, such as those of the peptide NAPVSIPQ, which binds to two iron sites and exhibits strong chelation activity. Notably, this peptide is capable of crossing the blood brain barrier and may offer potential therapeutic benefits (Blat et al., 2008). These findings support the potential therapeutic application of W-I1h. Consistent with these findings, the iron chelating activity of W-I1h (10,500 μg/mL) exceeded that of W-G, aligning with previous reports on hydrolysates such as phosvitin peptides from fresh egg yolk and *Tetraselmis chuii* microalgae, where intestinal-phase hydrolysates displayed superior iron chelation compared to gastric-phase hydrolysates (Moon & Cho, 2023; Song et al., 2023). Furthermore, the antioxidant activity of the INFOGEST control (enzyme and fluid-only samples) was negligible, confirming that the assay results were not confounded by fluids.

While iron and copper chelation share a common transition metal chelation mechanism, Santos et al. (2017) reported that iron chelating activity does not strongly correlate with copper chelating activity. For instance, while the iron chelating rates of B-G and B-I were comparable, the copper chelating activity of B-G at high concentrations (191–381 μg/mL) was significantly greater than B-I (Fig. 3). Interestingly, at lower concentrations (95–191 μg/mL), B-I1h demonstrated the highest copper chelating activity among all digestion stages, but this effect diminished

at higher concentrations. The copper chelating activity of W-I2h observed in this study is comparable to that of soy protein hydrolysates obtained via alcalase hydrolysis (~60 %) and pea protein hydrolysates obtained using alcalase and flavourzyme (~65 %) (El Hajj et al., 2023), while B-I2h is comparable to oat protein concentrate gastrointestinal digestates (49.4 %) (Sánchez-Velázquez, Cuevas-Rodríguez, et al., 2021).

3.2.2. ABTS and DPPH scavenging activity

Antiradical activity against ABTS was observed in both W and B digestates at all digestion stages (Fig. 4). In general, the ABTS inhibition activities of gastrointestinal digestates were higher than those observed for gastric digestates for both insects. Similar findings were reported by Khalesi and FitzGerald (2021) in soy protein, where ABTS scavenging activity after gastric digestion (EC_{50} = 0.31 mg/mL) was lower than after gastrointestinal digestion (EC_{50} = 0.19 mg/mL). This trend can be attributed to the progressive digestion process, which generates more dipeptides and smaller peptides fragments. These smaller peptides are more hydrophilic than larger peptides, allowing them to interact more effectively with the water-soluble ABTS radical (Zhu et al., 2008). The ABTS inhibition rates of W-I2h and B-I2h were 40.2 % and 49.8 %, respectively, which were lower than the 60.0 % inhibition observed with 1 mg/mL whey protein digestate produced using the INFOGEST protocol (de Espindola et al., 2023). The ABTS inhibition observed in this study is comparable to that reported for yam protein gastrointestinal digestates, which ranges between ~40 % and 55 % (do Nascimento et al., 2021).

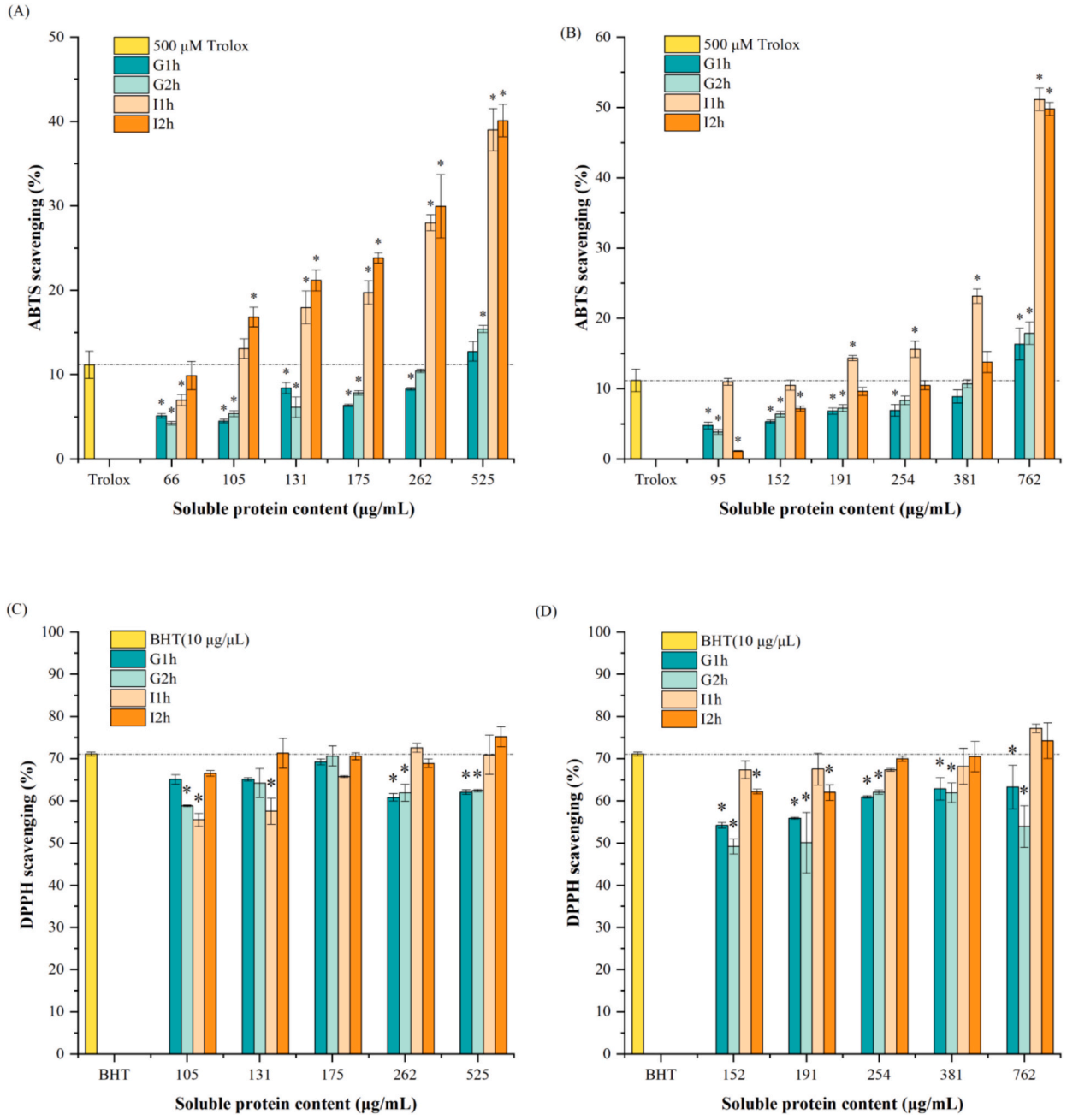

Fig. 4. Dose dependent inhibition of ABTS radical (%) of (A) Waxworm protein digestates and (B) Buffalo worm protein digestates derived from gastric and intestinal phases 1 h and 2 h (G1h, G2h, I1h, I2h). DPPH inhibition (%) of (C) Waxworm protein digestates; and (D) Buffalo worm protein digestates derived from gastric and intestinal phases 1 h and 2 h (G1h, G2h, I1h, I2h). * Means significant difference ($p < 0.05$) compared to the 500 μM Trolox or BHT (10 μg/mL) control, Tukey test. Data are mean with SD of triplicates.

The DPPH scavenging activity assay, which is based on a combination of electron transfer and hydrogen atom transfer mechanisms, showed trends similar to those observed for ABTS inhibition. In this study, gastrointestinal digestates (W-I and B-I) exhibited higher DPPH scavenging activity compared to gastric digestates (W-G and B-G) (Fig. 3). This enhanced activity may indicate that free amino acids and soluble peptides are effective donors of electrons and hydrogen atoms. Similar conclusions were drawn for legume paste gastrointestinal digestates, where gastrointestinal digestates showed superior electron and hydrogen atom donation abilities compared to gastric digestates (Gallego et al., 2020; Martínez-Villaluenga et al., 2024). The DPPH scavenging activities of both W-I2 and B-I2 at the highest concentrations were comparable to those of 20 mg/mL whey protein digestion-resistant peptides, which showed 75.1 % inhibition (de Espindola et al., 2023). Similarly, yam gastric and gastrointestinal digestates (10 mg – 20 mg sample/mL) showed DPPH radical scavenging activity ranging from ~50 % to ~70 % for gastric digestates and ~ 40 % to ~65 % for gastrointestinal digestates (do Nascimento et al., 2021).

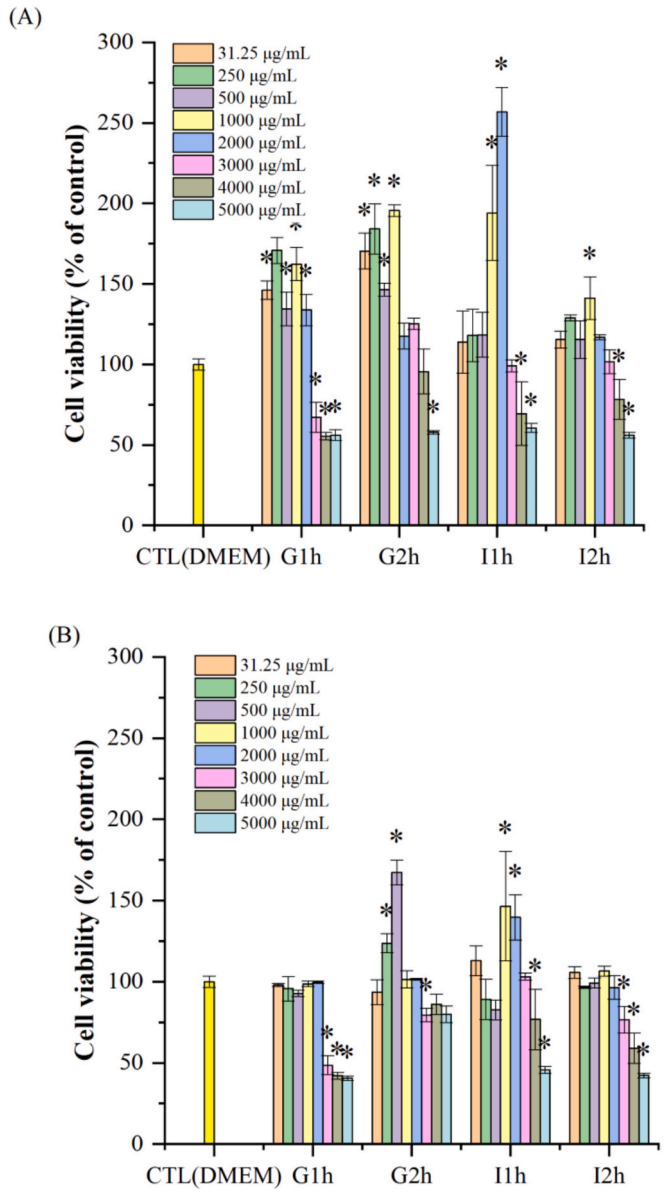

Fig. 5. Effects of the (A) Waxworm protein digestates and (B) Buffalo worm protein digestates below 10 kDa (31.25, 250, 500, 1000, 2000, 3000, 4000, 5000 μg soluble protein/mL) on Caco-2 cell viability. * Indicates significant differences ($p < 0.05$) between effects of individual treatments against the medium control (CTL). Data are mean with SD of three independent experiments in triplicates.

3.3. Insect protein digestate effects on intestinal cell viability

Prior to assessing the antioxidant activity and Caco-2 cells permeability, the cytotoxicity of insect protein-derived peptides (fractions <10 kDa) was evaluated using the MTS assay. As shown in Fig. 5, both insect digestates demonstrated similar behavior across all digestion stages. Gastrointestinal phase digestates, at specific concentrations (e.g., W-I1h 2000 and 1000 μg protein/mL; B-I1h 2000 and 1000 μg protein/mL), exhibited a tendency to produce fewer negative effects on the Caco-2 cells compared to gastric phase digestates. At higher concentrations, such as 5000 μg protein/mL and 4000 μg protein/mL, W-G, W-I, B-G and B-I reduced cell viability by 21.8 %–44.5 % and 13.9 %–58.0 %, respectively. Interestingly, toxicity was observed at 3000 μg protein/mL sample for W-G1h and B-G1h; however, this toxicity gradually decreased as digestion progressed, resulting in reduced cytotoxicity effects in later gastric phase digestates (2 h) and subsequent digestion stages. At concentrations below these thresholds, the digestates did not exhibit cytotoxic effects. Instead, some concentrations promoted cell proliferation, likely due to the release of free amino acids and smaller peptides during digestion. Proteolytic enzymes such as trypsin, pepsin, and chymotrypsin break down proteins into bioavailable peptides and free amino acids, which can be absorbed by Caco-2 cells and stimulate proliferation (Silk et al., 1985). Similarly, Dobermann and Scheers (2021) observed that insect digestates at specific protein concentrations promoted cell proliferation. For instance, at 0.333 mg protein/mL, cell viability was increased to 200 % and 150 %, for *G. bimaculatus* and *S. gregaria* digestates respectively. Based on these findings, a concentration of 2000 μg protein/mL was selected as the maximum concentration for subsequent cellular antioxidant assays (ROS and CAA assay) and peptide transepithelial transport studies. This concentration ensures minimal cytotoxic effects while allowing the evaluation of bioactive properties.

3.4. Insect protein digestate effects on cellular antioxidant activity

3.4.1. Cellular antioxidant activity (CAA) assay

The cellular antioxidant activity (CAA) assay evaluates the ability of antioxidant compounds, within a cellular environment, to inhibit the generation of peroxyl radical-induced oxidation of DCF, triggered by AAPH (Wolfe & Liu, 2007). This inhibition reflects the scavenging activity of the antioxidant substances.

To compare the antioxidant potential across treatments with varying concentrations, EC_{50} values and CAA units (%) were calculated and are summarized in Table 1. The EC_{50} values of B-G1h, B-I1h and B-I2h were 1.83 ± 3.90, 1.89 ± 12.88 and 1.86 ± 28.12 mg/mL, respectively, showing no statistic differences. This consistency may indicate that the primary antioxidant peptides in B were generated during the initial gastric digestion phase via pepsin hydrolysis. However, overreaction between pepsin and B digests during extended gastric digestion (B-G2h) may have resulted in the formation of pro-oxidative peptides. These pro-oxidative peptides were subsequently cleaved by chymotrypsin and trypsin during gastrointestinal digestion, restoring antioxidant activity to levels comparable to those observed at G1h (EC_{50} = 1.83 ± 3.90 mg/mL). In contrast, W digests from the gastrointestinal phase exhibited slightly lower EC_{50} values (I1h = 1.65 ± 8.60; I2h = 1.66 ± 5.74 mg/mL) compared to those from gastric phase. This suggests that the peptides collected from the gastrointestinal phase of W digestates enhanced antioxidant properties. Notably, the EC_{50} values of W during the gastric phase were statistically similar to all digestion stages of B digestates. Compared to reported values for corn peptides (2.85 mg/mL for <1 kDa fractions: 5.05 mg/mL for 1–3 kDa fractions), wild blueberry (2.53 mg/mL) and blackberry (3.19 mg/mL) (Ding et al., 2018; Wolfe et al., 2008),

Table 1
The median effective concentration (EC_{50}) and cellular antioxidant activity unit (CAA) values of insect derived peptide fractions (<10 kDa) from the different digestion stages. Different superscript letters within the same row are significantly different ($p < 0.05$), Tukey test.

	W				B			
	G1h	G2h	I1h	I2h	G1h	G2h	I1h	I2h
EC_{50} (mg/mL)	1.88 ± 2.35^{a}	1.79 ± 1.52^{a}	1.65 ± 8.60^{b}	1.66 ± 5.74^{b}	1.88 ± 3.90^{a}	_	1.85 ± 4.11^{a}	1.89 ± 5.41^{a}
CAA unit (%)	15.01 ± 1.95^{b}	13.59 ± 3.69^{d}	15.62 ± 0.48^{bc}	10.92 ± 1.67^{d}	12.43 ± 2.82^{cd}	_	19.25 ± 0.57^{a}	16.01 ± 1.66^{ab}

Note: The CAA unit (%) are calculated from the most effective concentration at each digestion stage. B-G2h showed peroxidation effects, data not shown.

the EC_{50} values of both W and B digests across all digestion stages were lower, demonstrating superior antioxidant activity. Moreover, the CAA unit (%) values were comparable to those of ungerminated chickpea gastrointestinal digestates (10 μg/mL = 10 %, 50 μg/mL = 20 %) (Newton & Majumder, 2023). These variations are likely attributable to the intrinsic differences in the dominant antioxidant peptides presents within each fraction, reflecting the unique peptide profiles and their respective contributions to antioxidant activity. The antioxidant activity exhibited by the digestates may be attributed to the primary structural properties of the protein concentrates, specifically their amino acid composition and sequence. Amino acids with strong antioxidant properties, including tryptophan, methionine, histidine, lysine, cysteine, arginine, and tyrosine, are likely key contributors to the observed activity in the generated peptides (Xu et al., 2017). Previous studies have reported that these amino acids constitute 23.6 % and 22.9 % of the total amino acid content in W protein concentrate and B protein concentrate, respectively (Ma, Mondor, Dowle, et al., 2024; Ma, Mondor, Goycoolea, et al., 2024). Furthermore, identified peptides such as FGPISIGNPPQSF, DAFPEQALDPINKPTF, PEQALDPINKPTFW and GGSAASLGDHPHLGG LL showed high antioxidant potential, which may contribute to the elevated antioxidant activity reported in this study.

3.5. Intracellular antioxidant activity (ROS)

The cellular antioxidant activity (CAA) assay, quantifies the total antioxidant effects both intracellularly and extracellularly. The antioxidant peptides absorbed by Caco-2 cells inhibit the generation of intracellular peroxyl radicals by AAPH. Simultaneously, AAPH generates radicals extracellularly, which can be scavenged by antioxidant peptides that have not been absorbed by the Caco-2 cells (Wolfe & Liu, 2007). To specifically assess the intracellular radical scavenging effects of W and B digestates, extracellular reactions between unabsorbed peptides and oxygen radicals were eliminated by washing the cells, isolating the intracellular antioxidant activity.

As shown in Fig. 6, the intracellular antioxidant activity of W and B digestates exhibited a dose-dependent behavior. Among the W digestates, only W-I1h (2.0 mg protein/mL) did not show significant inhibition effects compared to the control (CTL). All other concentrations and digestion stages (G1h, G2h, I2h) demonstrated significant inhibition of oxygen radicals generated by H_2O_2. Interestingly, B-I1h (2.0 mg protein/mL) also did not show a significant difference when compared to the control. This may be attributed to the promotion of cell growth by W and B I1h digestates at 2.0 mg protein/mL, which increased cell viability by almost 1.5 times to 2.5 times (Fig. 5). This proliferation likely resulted in the absorption of more H_2O_2 and the generation of additional oxygen radicals. For lower concentrations of W-I1h and B-I1h (1.75 mg protein/mL), generation rates of 86.9 % and 68.4 %, respectively, were observed. This suggests that lower concentrations of digestates at specific digestion stages may effectively scavenge radicals. Consistent with extracellular antioxidant activity, W-I2h demonstrated the highest intracellular ROS scavenging capacity. In comparison, the % inhibition for W-G1h was significantly lower than for W-I2h, supporting the hypothesis that peptides generated after one hour of gastric digestion are larger and less capable of entering Caco-2 cells to exhibit antioxidant effects (Ozorio et al., 2020).

The ROS scavenging capacity observed in this study aligns with

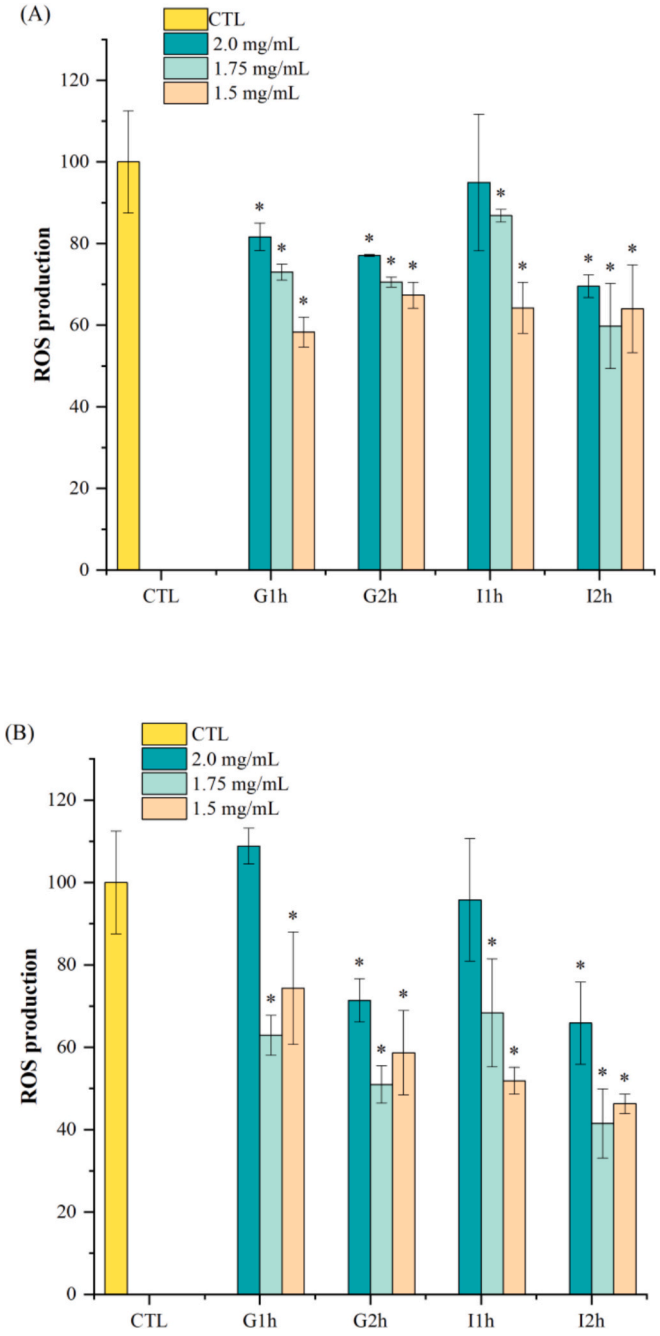

Fig. 6. Effects of insect digestates on inhibition of intracellular ROS formation 1 h (A) Waxworm protein digestates and (B) Buffalo worm protein digestates (<10 kDa) at gastric and intestinal phases 1 h and 2 h (G1h, G2h, I1h, I2h) under the Caco-2 cells oxidative stress condition induced by H_2O_2. * Means significant difference ($p < 0.05$) compared to control, Tukey test. Data are mean with SD of three independent experiments in triplicates.

reports on food-derived peptides, such as whey peptides and corn peptides (de Espindola et al., 2023; Ding et al., 2018; Wang et al., 2016). Similar, W-I2h and B-I2h digestates at lower concentrations (1.75 and 1.5 mg/mL) also exhibited the highest ROS inhibition rates (40.21 % and 58.5 %, respectively). The ROS inhibition rates of digested amaranth proteins <5 kDa (84.7 %) and >5 kDa (84.6 %) during the gastrointestinal phase (Serena-Romero et al., 2023), and ROS inhibition rates of digested British chia globulin 32 % (Wang et al., 2024). These results further demonstrating the antioxidant potential of insect-derived peptides.

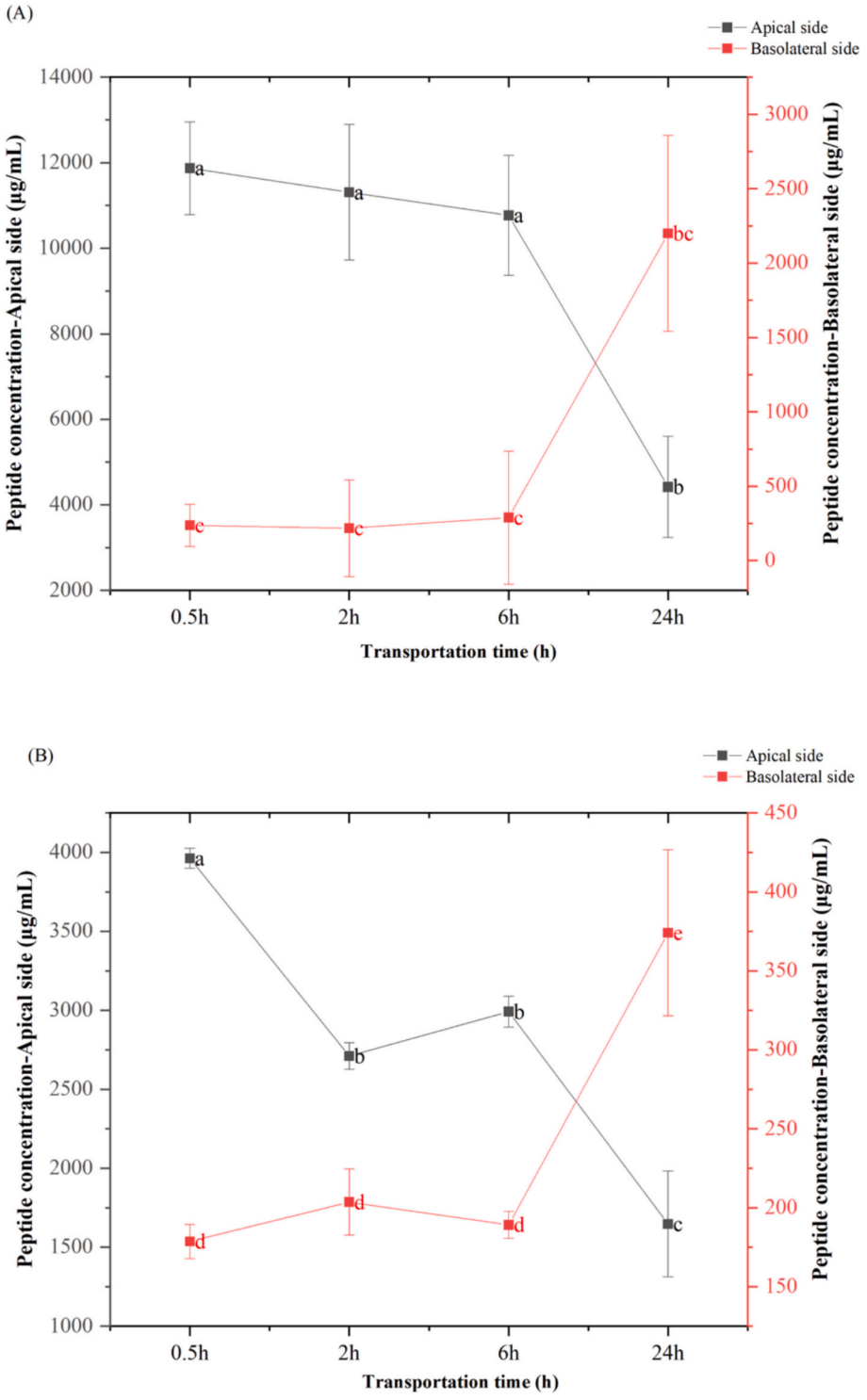

Fig. 7. The kinetics of permeable peptides at different time points as tested by Caco-2 monolayer transepithelial transport model. (A) The Waxworm intestinal 2 h digestates (W-I2h) permeable peptide content (μg/mL) in basolateral side and non-permeable peptide content (μg/mL) in apical side. (B) The Buffalo worm intestinal 2 h digestates (B-I2h) permeable peptide content (μg/mL) in basolateral side and non-permeable peptide content (μg/mL) in apical side. Different letters indicates significant differences ($p < 0.05$). Data are mean with SD of three independent experiments in triplicates.

Table 2
Apparent permeability (P_{app}) of W-I2h and B-I2h peptides from 0.5, 2, 6, 24 h transepithelial transport.

Time (h)	P_{app} – W (cm/s)	P_{app} – B (cm/s)
0.5–2 h	$1.49 \times 10^{-6} \pm 0.52^{a}$	$9.53 \times 10^{-7} \pm 1.08^{c}$
2–6 h	$1.03 \times 10^{-6} \pm 0.28^{a}$	$2.17 \times 10^{-7} \pm 1.42^{d}$
6–24 h	$6.10 \times 10^{-6} \pm 0.32^{b}$	$5.91 \times 10^{-7} \pm 0.31^{e}$

3.6. Transepithelial transport of insect protein-derived peptides

Food derived peptides are known for their low bioavailability and limited correlation with *in vitro* activity assays. To address this limitation, a Caco-2 monolayer model was applied as an *in vitro* absorption model to simulate the human small intestinal epithelium. This epithelium consists of well-differentiated, polarized cells with tight junctions, serving as protective barrier against external environment while facilitating primary nutrient absorption (Marchiando et al., 2010).

In this study, Caco-2 cells were grown for 21 days to develop semi-permeable monolayers with functional tight junctions. These monolayers exhibited key intestinal epithelium characteristics such as cell polarity, microvilli formation, brush-border membrane enzymes, receptors and transport carriers (Hidalgo et al., 1989). The model includes more than 8 types of membrane peptidases that hydrolyze oligopeptides into shorter peptides and free amino acids. Among these, dipeptidyl peptidase (DPP-IV) has demonstrated the highest activity and is mainly responsible for cleaving N-terminus substrates such as peptides, protein or peptide-like molecules (Aertgeerts et al., 2004). Combined with the INFOGEST model, this system replicates two critical barriers in peptide absorption: enzymatic degradation during gastrointestinal digestion and transepithelial permeability through the intestinal epithelium. Artursson et al. (2001) confirmed the strong correlation between Caco-2 monolayer transport and *in vivo* absorption.

Based on cell viability assays, gastrointestinal 2 h digestates at 2000 μg protein/mL were not toxic to Caco-2 cells and were selected for transepithelial transport analysis. The kinetics of peptide transport across the Caco-2 monolayer were evaluated at different time intervals (Fig. 7). Both insect digestates showed similar permeable peptide kinetics, with the most peptides permeating across the Caco-2 monolayer between 6 h and 24 h, evidenced by a sharp increase in peptide content in basolateral compartment during this period. As for the apparent permeability coefficient (P_{app}) values, summarized in Table 2, in general, the P_{app} of W is higher compared to B. The P_{app} for W exceed 1×10^{-6} cm/s, reaching up to 6.10×10^{-6} cm/s between 6 and 24 h. In contrast, the P_{app} for B was lower, ranging between 1×10^{-6} cm/s and 1×10^{-7} cm/s. Yang et al. (2017) suggested that compounds with a $P_{app} > 1 \times 10^{-6}$ cm/s are completely absorbed, while those with a $P_{app} < 1 \times 10^{-7}$ cm/s exhibit incomplete absorption. This study represents the first report of insect-derived peptides permeating the Caco-2 monolayer. Compared to peptides from other food sources, the P_{app} of insect-derived peptides was higher than that of corn-derived peptides YFCLT and GLLLPH (1.10×10^{-7} and 1.98×10^{-7} cm/s, respectively), suggesting that insect-derived peptides can traverse the cell membrane more efficiently than corn-derived peptides (Ding et al., 2018). However, the P_{app} of W peptides was lower than that of bovine milk-derived peptides, which range from 0.57 to 9.21×10^{-6} cm/s (Sienkiewicz-Szłapka et al., 2009), suggesting that milk-derived peptides exhibit greater permeability. These findings indicate that insect-derived peptides can be absorbed by the human digestive system, with W peptides showing the highest absorption between 6 and 24 h.

3.7. Identification of peptides after gastrointestinal digestion and transepithelial transport

Peptides collected from the final stage of gastrointestinal digestion (I2h) and from the basolateral side (at 6 h and 24 h transport) were subjected to DDA-PASEF, LC-MS/MS analysis for sequence characterization. The identified peptides are listed in Appendix table. Previous studies have reported that Caco-2 cells can absorb peptides consisting of up to 26 amino acids. The transportation of peptides across the intestinal epithelium occurs via multiple mechanisms, like 'transporter-mediated transport, transcellular passive diffusion, and paracellular transport' (Liang et al., 2018). According to the molecular weight, high-molecular weight peptides (1600–500 Da) are primarily transported by paracellular transport involving transcytosis. In this study, most of the identified peptides from the I2h and basolateral side samples (at 6 h and 24 h transport) fell within 1600–500 Da range, suggesting that their likely transportation mechanism was paracellular transport with transcytosis (Fan et al., 2022; Imani et al., 2022). These peptides interact with tight junctions or epithelial cells to facilitate transport across the intestinal barrier. A comparison of peptide transport at 6 h and 24 h revealed notable differences (Fig. 8). At 6 h, 430 peptides from W and 222 peptides from (B) crossed the Caco-2 monolayer, whereas at 24 h, 5888 from W and 574 peptides from B were transported (Fig. 8). Furthermore, the peptide lengths also differed significantly between the two time points. At 24 h, the peptides were generally shorter than those at 6 h, attributed to the additional hydrolysis by intestinal peptidases and proteases. Peptidases are known to cleave peptides by removing one amino acid at a time from the peptide chain. For instance, the peptide VALDFEQEMATAASSSSLEK identified at 6 h was further processed to DFEQEMATAASSSSLEK at 24 h, highlighting the activity of peptidases. On the other hand, peptides with aromatic amino acids such as Phe, Tyr, Pro and Trp at their C-terminal and N-terminal are less susceptible to

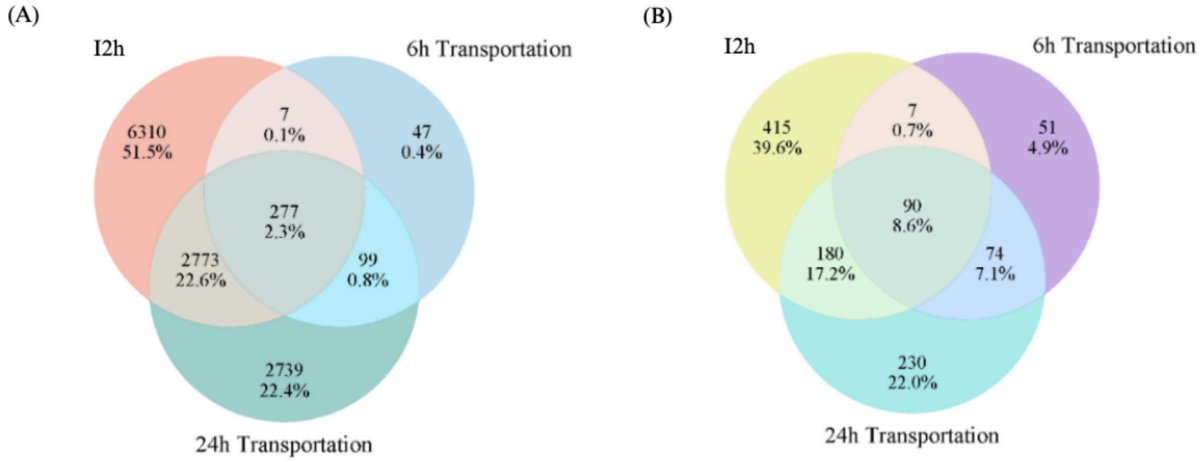

Fig. 8. Presence of the common and unique peptides in the basolateral fraction after 6 and 24 h exposure. (A) Waxworm (B) Buffalo worm.

degradation by peptidases and proteases. This trend was consistent in the present study, where peptides lacking these aromatic residues at their termini (e.g., LHFFMPGFAPLTSR, VSTGGGASLELLEGK, ADQLTEEQIAEFK) were more prone to hydrolysis and were not detected at 24 h transport. These findings align with the established theory of peptide stability concerning terminal residues, providing insight into the absorption dynamics of insect-derived peptides.

4. Conclusion

In summary, Waxworm and Buffalo worm proteins were subjected to *in vitro* digestion for the first time to our knowledge using the INFOGEST model, and their transepithelial transport was simulated. The antioxidant activity of peptides generated during gastric and gastrointestinal digestion was evaluated using both *in vitro* and cellular assays. The *in vitro* results showed that both W-I and B-I digestates exhibited enhanced transition metal chelating activity (Fe^{2+} and Cu^{2+}) and radical scavenging activities (ABTS and DPPH) compared to their gastric counterparts (W-G and B-G), with scavenging activities being largely dose-dependent. Interestingly, W-I1h appeared to contain peptides particularly effective at iron chelation, with the highest percentage chelation observed. The transepithelial transport analysis revealed that peptides from W exhibited a higher p_{app} (6.10×10^{-6} cm/s) compared to B (5.91×10^{-7} cm/s). This resulted in a higher peptide concentration in the basolateral side for W (24 h = 2199.9 μg peptides/mL), compared to B (24 h = 374.1 μg peptides/mL). These permeability results corresponded to the findings from the ROS and CAA assays. Specifically, W-I2h demonstrated superior ROS scavenging activity (inhibition = 40.2 %) compared to B-I2h (inhibition = 58.5 %). Similarly, W-I2h exhibited the lowest EC_{50} value (1.66 mg/mL) in the CAA assay, indicating higher antioxidant potential. This study represents the first comprehensive analysis and identification of antioxidant peptides derived from Waxworm and Buffalo worm proteins following digestion, along with their associated permeability. These findings underscore the antioxidant potential of W and B, providing a foundation for future research into the potential health benefits of insect-derived peptides and their applications as functional foods and nutraceuticals. The antioxidant activity of W and B peptides is comparable to other insects-peptides, and surpasses that of plant-derived peptides. The next step of this study will involve a more in-depth investigation into the additional biological activities of the peptides generated during digestion, particularly their antioxidant-related functions, such as anti-inflammatory properties and their potential role in mitigating inflammation.

CRediT authorship contribution statement

Zidan Ma: Writing – original draft, Visualization, Validation, Methodology, Investigation, Formal analysis, Data curation, Conceptualization. **Martin Mondor:** Writing – review & editing, Visualization, Validation, Supervision, Investigation. **Christine Boesch:** Writing – review & editing, Visualization, Validation, Supervision, Methodology. **Oscar Abel Sánchez-Velázquez:** Writing – review & editing, Methodology, Investigation. **Adam A. Dowle:** Writing – review & editing, Software, Methodology, Formal analysis, Data curation. **Alan Javier Hernández-Álvarez:** Writing – review & editing, Visualization, Validation, Supervision, Resources, Project administration, Investigation, Funding acquisition, Data curation, Conceptualization.

Declaration of competing interest

The authors declare that they have no known competing financial interests or personal relationships that could have appeared to influence the work reported in this paper.

Acknowledgements

This work is supported by the University of Leeds, School of Food Science and Nutrition, United Kingdom (Grant number: 95522790). This work was funded by the UK National Alternative Proteins Innovation Centre (NAPIC), which is an Innovation and Knowledge Centre funded by the Biotechnology and Biological Sciences Research Council and Innovate UK (Grant Ref: BB/Z516119/1).

Appendix A. Supplementary data

Supplementary data to this article can be found online at https://doi.org/10.1016/j.foodchem.2025.144036.

Data availability

No data was used for the research described in the article.

References

Abeyrathne, E. D. N. S., Nam, K., Huang, X., & Ahn, D. U. (2022). Plant-and animal-based antioxidants' structure, efficacy, mechanisms, and applications: A review. *Antioxidants, 11*(5), 1025.

Aertgeerts, K., Ye, S., Tennant, M. G., Kraus, M. L., Rogers, J., Sang, B. C., … Prasad, G. S. (2004). Crystal structure of human dipeptidyl peptidase IV in complex with a decapeptide reveals details on substrate specificity and tetrahedral intermediate formation. *Protein Science, 13*(2), 412–421.

Amigo, L., & Hernández-Ledesma, B. (2020). Current evidence on the bioavailability of food bioactive peptides. *Molecules, 25*(19), 4479.

Araiza-Calahorra, A., Mondor, M., Boesch, C., Orfila, C., Goycoolea, F. M., & Hernández-Álvarez, A. J. (2022). Proteins, peptides, and protein hydrolysates as immunomodulatory and antioxidant agents for the formulation of functional foods. In *Current advances for development of functional foods modulating inflammation and oxidative stress* (pp. 137–164). Elsevier.

Artursson, P., Palm, K., & Luthman, K. (2001). Caco-2 monolayers in experimental and theoretical predictions of drug transport. *Advanced Drug Delivery Reviews, 46*(1–3), 27–43.

Blat, D., Weiner, L., Youdim, M. B., & Fridkin, M. (2008). A novel iron-chelating derivative of the neuroprotective peptide NAPVSIPQ shows superior antioxidant and antineurodegenerative capabilities. *Journal of Medicinal Chemistry, 51*(1), 126–134.

Brodkorb, A., Egger, L., Alminger, M., Alvito, P., Assunção, R., Ballance, S., Bohn, T., Bourlieu-Lacanal, C., Boutrou, R., & Carrière, F. (2019). INFOGEST static in vitro simulation of gastrointestinal food digestion. *Nature Protocols, 14*(4), 991–1014.

Canabady-Rochelle, L. L., Harscoat-Schiavo, C., Kessler, V., Aymes, A., Fournier, F., & Girardet, J.-M. (2015). Determination of reducing power and metal chelating ability of antioxidant peptides: Revisited methods. *Food Chemistry, 183*, 129–135.

Carrasco-Castilla, J., Hernández-Álvarez, A. J., Jiménez-Martínez, C., Jacinto-Hernández, C., Alaiz, M., Girón-Calle, J., … Dávila-Ortiz, G. (2012). Antioxidant and metal chelating activities of Phaseolus vulgaris L. var. Jamapa protein isolates, phaseolin and lectin hydrolysates. *Food Chemistry, 131*(4), 1157–1164.

Ding, L., Wang, L., Zhang, T., Yu, Z., & Liu, J. (2018). Hydrolysis and transepithelial transport of two corn gluten derived bioactive peptides in human Caco-2 cell monolayers. *Food Research International, 106*, 475–480.

Dobermann, D., & Scheers, N. (2021). *Cytotoxicity of insects (T. molitor, G. Bimaculatis, S. gregaria and A. domesticus) in A simulated gastrointestinal digestion/human intestinal cell model*.

El Hajj, S., Irankunda, R., Echavarría, J. A. C., Arnoux, P., Paris, C., Stefan, L., … Canabady-Rochelle, L. (2023). Metal-chelating activity of soy and pea protein hydrolysates obtained after different enzymatic treatments from protein isolates. *Food Chemistry, 405*, Article 134788.

de Espindola, J. S., Taccóla, M. F., da Silva, V. S. N., Dos Santos, L. D., Rossini, B. C., Mendonça, B. C., … Galland, F. (2023). Digestion-resistant whey peptides promote antioxidant effect on Caco-2 cells. *Food Research International, 173*, Article 113291.

Fan, H., Liu, H., Zhang, Y., Zhang, S., Liu, T., & Wang, D. (2022). Review on plant-derived bioactive peptides: Biological activities, mechanism of action and utilizations in food development. *Journal of Future Foods, 2*(2), 143–159.

Finkel, T., & Holbrook, N. J. (2000). Oxidants, oxidative stress and the biology of ageing. *Nature, 408*(6809), 239–247.

Gallego, M., Arnal, M., Barat, J. M., & Talens, P. (2020). Effect of cooking on protein digestion and antioxidant activity of different legume pastes. *Foods, 10*(1), 47.

Gruppi, A., Dermiki, M., Spigno, G., & FitzGerald, R. J. (2022). Impact of enzymatic hydrolysis and heat inactivation on the physicochemical properties of milk protein hydrolysates. *Foods, 11*(4), 516.

Hall, F. G., Jones, O. G., O'Haire, M. E., & Liceaga, A. M. (2017). Functional properties of tropical banded cricket (Gryllodes sigillatus) protein hydrolysates. *Food Chemistry, 224*, 414–422.

Han, R., Álvarez, A. J. H., Maycock, J., Murray, B. S., & Boesch, C. (2021). Comparison of alcalase-and pepsin-treated oilseed protein hydrolysates–experimental validation of predicted antioxidant, antihypertensive and antidiabetic properties. *Current Research in Food Science, 4*, 141–149.

Hidalgo, I. J., Raub, T. J., & Borchardt, R. T. (1989). Characterization of the human colon carcinoma cell line (Caco-2) as a model system for intestinal epithelial permeability. *Gastroenterology, 96*(2), 736–749.
Hubatsch, I., Ragnarsson, E. G., & Artursson, P. (2007). Determination of drug permeability and prediction of drug absorption in Caco-2 monolayers. *Nature Protocols, 2*(9), 2111–2119.
Imani, S., Alizadeh, A., Tabibiazar, M., Hamishehkar, H., & Roufegarinejad, L. (2022). Nanoliposomal co-encapsulation of cinnamon extract and zein hydrolysates with synergistic antioxidant activity for nutraceutical applications. *Chemical Papers, 76*(4), 2059–2069.
Kellett, M. E., Greenspan, P., & Pegg, R. B. (2018). Modification of the cellular antioxidant activity (CAA) assay to study phenolic antioxidants in a Caco-2 cell line. *Food Chemistry, 244*, 359–363.
Khalesi, M., & FitzGerald, R. J. (2021). In vitro digestibility and antioxidant activity of plant protein isolate and milk protein concentrate blends. *Catalysts, 11*(7), 787.
Kotha, R. R., Tareq, F. S., Yildiz, E., & Luthria, D. L. (2022). Oxidative stress and antioxidants—A critical review on in vitro antioxidant assays. *Antioxidants, 11*(12), 2388.
Liang, Q., Chalamaiah, M., Ren, X., Ma, H., & Wu, J. (2018). Identification of new anti-inflammatory peptides from zein hydrolysate after simulated gastrointestinal digestion and transport in Caco-2 cells. *Journal of Agricultural and Food Chemistry, 66*(5), 1114–1120.
Ma, Z., Mondor, M., Dowle, A. A., Goycoolea, F. M., & Hernández-Álvarez, A. J. (2024). Buffalo worm (Alphitobius diaperinus) proteins: Structural properties, proteomics and nutritional benefits. *Food Chemistry, 141757*.
Ma, Z., Mondor, M., Goycoolea, F. M., Ganji, S. R., & Hernández-Álvarez, A. J. (2024). Unlocking the potential of waxworm (galleria mellonella) proteins: Extraction, fractionation, and protein quality assessment. *Food Bioscience, 59*, Article 103955.
Ma, Z., Mondor, M., Valencia, F. G., & Hernández-Álvarez, A. J. (2023). Current state of insect proteins: Extraction technologies, bioactive peptides and allergenicity of edible insect proteins. *Food &, function(14)*, 8129–8156.
Marchiando, A. M., Graham, W. V., & Turner, J. R. (2010). Epithelial barriers in homeostasis and disease. *Annual Review of Pathology: Mechanisms of Disease, 5*, 119–144.
Martínez-Villaluenga, C., Peñas, E., Mondor, M., Han, R., & Hernandez-Alvarez, A. J. (2024). Bioactive peptides released from legumes during gastrointestinal digestion. In *Protein Digestion-Derived Peptides* (pp. 261–303). Elsevier.
Moon, S.-H., & Cho, S.-J. (2023). Evaluation of the antioxidant activity of Tetraselmis chuii after in vitro gastrointestinal digestion and investigation of its antioxidant peptides. *Algal Research, 76*, Article 103328.
do Nascimento, E. S., Anaya, K., de Oliveira, J. M. C., de Lacerda, J. T. J. G., Miller, M. E., Dias, M., … Juliano, M. A. (2021). Identification of bioactive peptides released from in vitro gastrointestinal digestion of yam proteins (Dioscorea cayennensis). *Food Research International, 143*, Article 110286.
Newton, A., & Majumder, K. (2023). Germination and simulated gastrointestinal digestion of chickpea (Cicer arietinum L.) in exhibiting in vitro antioxidant activity in gastrointestinal epithelial cells. *Antioxidants, 12*(5), Article 1114.
Njoya, E. M. (2021). Medicinal plants, antioxidant potential, and cancer. In *Cancer* (pp. 349–357). Elsevier.
Ozorio, L., Mellinger-Silva, C., Cabral, L. M., Jardin, J., Boudry, G., & Dupont, D. (2020). The influence of peptidases in intestinal brush border membranes on the absorption of oligopeptides from whey protein hydrolysate: An ex vivo study using an ussing chamber. *Foods, 9*(10), Article 1415.
Pizzino, G., Irrera, N., Cucinotta, M., Pallio, G., Mannino, F., Arcoraci, V., Squadrito, F., Altavilla, D., & Bitto, A. (2017). Oxidative stress: Harms and benefits for human health. *Oxidative Medicine and Cellular Longevity, 2017*, Article 8146763.
Prior, R. L., Wu, X., & Schaich, K. (2005). Standardized methods for the determination of antioxidant capacity and phenolics in foods and dietary supplements. *Journal of Agricultural and Food Chemistry, 53*(10), 4290–4302.
Re, R., Pellegrini, N., Proteggente, A., Pannala, A., Yang, M., & Rice-Evans, C. (1999). Antioxidant activity applying an improved ABTS radical cation decolorization assay. *Free Radical Biology and Medicine, 26*(9–10), 1231–1237.
Roosenberg, J. M., II, Lin, Y.-M., Lu, Y., & Miller, M. J. (2000). Studies and syntheses of siderophores, microbial iron chelators, and analogs as potential drug delivery agents. *Current Medicinal Chemistry, 7*(2), 159–197.
Sánchez-Velázquez, O. A., Cuevas-Rodríguez, E. O., Mondor, M., Ribéreau, S., Arcand, Y., Mackie, A., & Hernández-Álvarez, A. J. (2021). Impact of in vitro gastrointestinal digestion on peptide profile and bioactivity of cooked and non-cooked oat protein concentrates. *Current Research in Food Science, 4*, 93–104.
Sánchez-Velázquez, O. A., Mulero, M., Cuevas-Rodríguez, E. O., Mondor, M., Arcand, Y., & Hernández-Álvarez, A. J. (2021). In vitro gastrointestinal digestion impact on stability, bioaccessibility and antioxidant activity of polyphenols from wild and commercial blackberries (Rubus spp.). *Food & Function, 12*(16), 7358–7378.
Sánchez-Velázquez, O. A., Ribéreau, S., Mondor, M., Cuevas-Rodríguez, E. O., Arcand, Y., & Hernández-Álvarez, A. J. (2021). Impact of processing on the in vitro protein quality, bioactive compounds, and antioxidant potential of 10 selected pulses. *Legume Science, 3*(2), Article e88.
Santos, J. S., Brizola, V. R. A., & Granato, D. (2017). High-throughput assay comparison and standardization for metal chelating capacity screening: A proposal and application. *Food Chemistry, 214*, 515–522.
Seifried, H. E., Anderson, D. E., Fisher, E. I., & Milner, J. A. (2007). A review of the interaction among dietary antioxidants and reactive oxygen species. *The Journal of Nutritional Biochemistry, 18*(9), 567–579.
Serena-Romero, G., Ignot-Gutiérrez, A., Conde-Rivas, O., Lima-Silva, M. Y., Martínez, A. J., Guajardo-Flores, D., & Cruz-Huerta, E. (2023). Impact of in vitro digestion on the digestibility, amino acid release, and antioxidant activity of Amaranth (Amaranthus cruentus L.) and Cañihua (Chenopodium pallidicaule Aellen) proteins in Caco-2 and HepG2 cells. *Antioxidants, 12*(12), Article 2075.
Sienkiewicz-Szłapka, E., Jarmołowska, B., Krawczuk, S., Kostyra, E., Kostyra, H., & Bielikowicz, K. (2009). Transport of bovine milk-derived opioid peptides across a Caco-2 monolayer. *International Dairy Journal, 19*(4), 252–257.
Silk, D., Grimble, G., & Rees, R. (1985). Protein digestion and amino acid and peptide absorption. *Proceedings of the Nutrition Society, 44*(1), 63–72.
Song, L., Zhu, L., Qiao, S., Song, L., Zhang, M., Xue, T., Lv, B., Liu, H., & Zhang, X. (2023). Preparation, characterization, and bioavailability evaluation of antioxidant phosvitin peptide-ferrous complex. *Journal of the Science of Food and Agriculture*, 3090–3099.
Udenigwe, C. C., & Aluko, R. E. (2012). Food protein-derived bioactive peptides: Production, processing, and potential health benefits. *Journal of Food Science, 77*(1), R11–R24.
Wang, L., Ding, L., Yu, Z., Zhang, T., Ma, S., & Liu, J. (2016). Intracellular ROS scavenging and antioxidant enzyme regulating capacities of corn gluten meal-derived antioxidant peptides in HepG2 cells. *Food Research International, 90*, 33–41.
Wang, X., Le, B., Zhang, N., Bak, K. H., Zhang, Y., & Fu, Y. (2023). Off-flavour compounds in collagen peptides from fish: Formation, detection and removal. *International Journal of Food Science & Technology, 58*(3), 1543–1563.
Wang, Y., Hernández-Alvarez, A. J., Goycoolea, F. M., & Martínez-Villaluenga, C. (2024). A comparative study of the digestion behavior and functionality of protein from chia (Salvia hispanica L.) ingredients and protein fractions. *Current research in food. Science, 8*, Article 100684.
Wolfe, K. L., Kang, X., He, X., Dong, M., Zhang, Q., & Liu, R. H. (2008). Cellular antioxidant activity of common fruits. *Journal of Agricultural and Food Chemistry, 56*(18), 8418–8426.
Wolfe, K. L., & Liu, R. H. (2007). Cellular antioxidant activity (CAA) assay for assessing antioxidants, foods, and dietary supplements. *Journal of Agricultural and Food Chemistry, 55*(22), 8896–8907.
Xiang, Z., Xue, Q., Gao, P., Yu, H., Wu, M., Zhao, Z., Li, Y., Wang, S., Zhang, J., & Dai, L. (2023). Antioxidant peptides from edible aquatic animals: Preparation method, mechanism of action, and structure-activity relationships. *Food Chemistry, 404*, Article 134701.
Xu, N., Chen, G., & Liu, H. (2017). Antioxidative categorization of twenty amino acids based on experimental evaluation. *Molecules, 22*(12), 2066.
Yang, Y., Zhao, Y., Yu, A., Sun, D., & Yu, L. (2017). Oral drug absorption: Evaluation and prediction. In *Developing solid oral dosage forms* (pp. 331–354). Elsevier.
Zhu, L., Chen, J., Tang, X., & Xiong, Y. L. (2008). Reducing, radical scavenging, and chelation properties of in vitro digests of alcalase-treated zein hydrolysate. *Journal of Agricultural and Food Chemistry, 56*(8), 2714–2721.
Żyżelewicz, D., Zakłos-Szyda, M., Juśkiewicz, J., Bojczuk, M., Oracz, J., Budryn, G., Miśkiewicz, K., Krysiak, W., Zduńczyk, Z., & Jurgoński, A. (2016). Cocoa bean (Theobroma cacao L.) phenolic extracts as PTP1B inhibitors, hepatic HepG2 and pancreatic β-TC3 cell cytoprotective agents and their influence on oxidative stress in rats. *Food Research International, 89*, 946–957.